Int. J. Heat Mass Transfer. Vol. 34, No. 7, pp. 1881–1894, 1991
Printed in Great Britain

0017–9310/91 $3.00+0.00

Evaporation of a liquid droplet on a hot plate

T. Y. XIONG† and M. C. YUEN
Department of Mechanical Engineering, Northwestern University, Evanston, IL 60208, U.S.A.

(*Received* 25 *June* 1990 *and in final form* 8 *August* 1990)

Abstract—The evaporation of a small liquid droplet impinging on a hot stainless steel plate is investigated. The liquids include water, various pure and mixed hydrocarbon fuels with drop sizes ranging from 0.07 to 1.8 mm. The wall temperatures varying from 63 to 605°C cover the entire spectrum of heat transfer characteristics from film evaporation (below boiling temperature) to spheroidal vaporization (above Leidenfrost temperature). A strobe–video visual system is used to record the transient process and to measure the droplet lifetime. Qualitatively, the droplet lifetime curve as a function of wall temperature is similar for all liquids and all drop sizes. The maximum heat transfer rate occurs at 50–60°C above the boiling temperature for all pure liquids and the Leidenfrost heat transfer rate occurs at about 120°C for pure fuels and 180°C for water above the boiling temperature. The maximum evaporation rate can significantly exceed the burning rate of fuel droplets. Visual observations show that beyond the maximum heat transfer point, larger droplets levitate above the surface whereas smaller droplets bounce up and down to many diameters above the surface. Thus for the smallest droplets beyond the Leidenfrost temperature, the droplet lifetime actually increases with wall temperature which is in contrast to the larger droplets. The maximum heat transfer rate is independent of drop sizes for all fuels and shows a small decrease with increasing drop sizes in the case of water. At the Leidenfrost temperature, the data show that the heat transfer rate is maximum at a droplet diameter of approximately 0.5 mm.

1. INTRODUCTION

THE EVAPORATION and ignition of liquid droplets impinging on a hot surface are of interest in a number of areas related to various types of combustion engines, cooling systems as well as many fire safety situations. In all of the above applications, the dynamic behavior of the impinging droplets, the heat and mass transfer between droplets and the hot surface, and the ignition characteristics of fuel droplets are important phenomena requiring fundamental investigation.

The first observation of the behavior of a droplet levitated over a hot, horizontal surface was reported by Leidenfrost in 1756 and hence the behavior is known as the Leidenfrost phenomenon. However, a systematic study of the phenomenon began much later with Tamura and Tanasawa [1]. They measured the evaporation lifetime of liquid droplets levitated over a hot surface at atmospheric pressure. As shown in Fig. 1, they classified the dynamics and heat transfer of droplet evaporation into four regimes: film evaporation (a–b), nucleate boiling (b–c), transition (c–d) and spheroidal vaporization (>d). The temperature at point b is the boiling temperature and at point d the Leidenfrost temperature, where the heat transfer reaches a local minimum. Of particular interest is point c where heat transfer is maximum. Since then much progress has been made in extending the work of ref. [1] (e.g. see refs. [2–12]). These include experimental studies, as well as theoretical and numerical analyses on the effect of ambient pressure, types of liquids, surface conditions (roughness, temperature and material) and initial drop sizes.

In all of the previous experimental studies, the impinging droplets were produced by a hypodermic syringe. Therefore, the droplet diameters were, in general, larger than 1 mm, which is much larger than the typical droplets in sprays. Because there exist significant effects of droplet sizes on the dynamics and thereby the thermochemistry of a droplet impinging

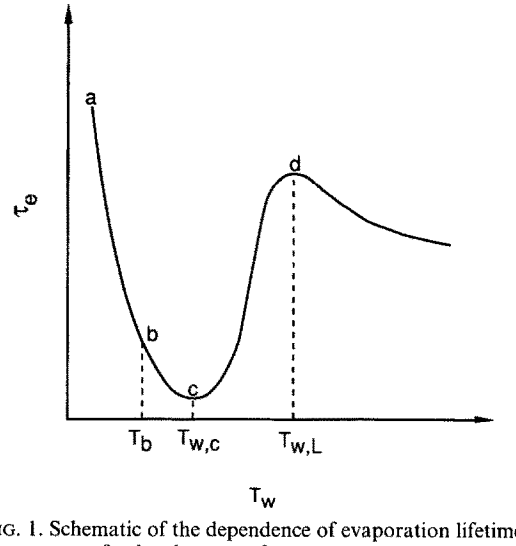

FIG. 1. Schematic of the dependence of evaporation lifetime of a droplet on surface temperature.

† Present address: Institute of Gas Technology, 3424 S. State St., Chicago, IL 60616, U.S.A.

NOMENCLATURE

a	radius
A_a	Antonie coefficient, equation (A5)
B	mass transfer number
B_a	Antonie coefficient, equation (A5)
C_a	Antonie coefficient, equation (A5)
c_p	specific heat at constant pressure
D_g	diffusion coefficient
D^*	equivalent diameter
D_0	initial droplet diameter
E_0	Eotros number, $g(\rho_l-\rho_g)D^{*2}/\sigma$
f	frequency
h	height
H	effective heat of vaporization, $L+c_p(T_d-T_\infty)$
L	latent heat of vaporization
$\dot{m}$	mass frequency rate
M	molecular weight
p	pressure
$\dot{q}$	heat transfer rate per unit area
T	temperature
U	velocity
V	volume
We	Weber number
y	distance above hot surface
Y	mass fraction.

Greek symbols

ρ	density
σ	surface tension
τ_e	droplet evaporation lifetime.

Subscripts

a	air
b	boiling
c	critical
d	droplet
g	gas
i	image
l	liquid
L	Leidenfrost
v	vapor
w	wall
0	initial
∞	ambient.

on a hot surface, applications of results obtained for larger droplets are limited.

The objective of the present study is to focus on droplets over a wide range of sizes with emphasis on smaller diameters comparable to droplet sizes in sprays. Diameters of the droplets produced in the present experiment range from 0.068 to 1.8 mm. A strobe–video visual system was developed to observe, record and measure the dynamics, evaporation and ignition of droplets.

2. EXPERIMENTS

In this section, the experiment and measurement technique will be briefly presented; the detail is described in ref. [13].

Figure 2 shows the schematic of the present experimental set-up. The hot plate consists of a rectangular (156 mm × 56 mm) 304 stainless steel plate with a thickness of 12.7 mm sitting on top of an electric heater with a power capacity of 450 W. Six pairs of chromel–alumel thin foil (0.013 mm thickness) thermocouples were cemented to both sides of the plate to measure both the surface temperatures as well as heat flux. The sides of the plate and heater are insulated. In addition, natural convection induced by the hot plate is restricted to be two-dimensional by installing two glass plates 90 mm in height along the long sides of the hot plate. As a result of insulation, surface temperature is uniform to within ±1% in a 20 mm square at the center of the plate. Examples of vertical temperature distribution above the plate along the centerline are shown in Fig. 3. As shown, there was a significant temperature variation within 10 mm above the surface. The vertical velocity profile at the center of the plate obtained by the LDV method is shown in Fig. 4. Figure 4 indicates that the vertical velocity reaches a maximum at about 6–10 mm above the hot plate. Since a small droplet can rebound to about 10 mm above the hot surface, it is expected that there is significant interaction between the droplet and natural convection.

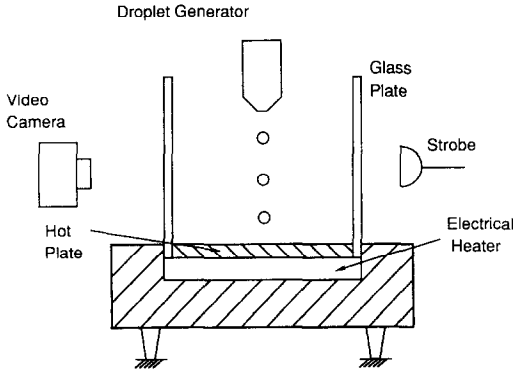

FIG. 2. Schematic of the experimental set-up.

The water-cooled droplet generator can be moved both vertically and horizontally to control precisely the location of the droplet impinging on the surface. Two droplet generators were used. For drop sizes between 0.068 and 0.45 mm the droplets were generated by the deformation of a piezoelectric element. This apparatus was adopted from the one developed by Wang [14]. For a larger droplet (above 0.4 mm

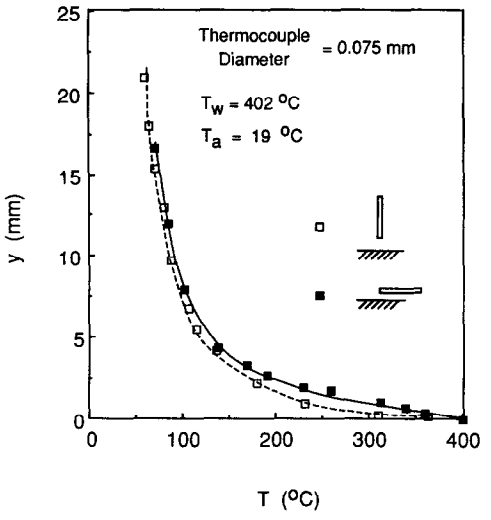

FIG. 3. Temperature profiles above the hot surface at $T_w = 402°C$.

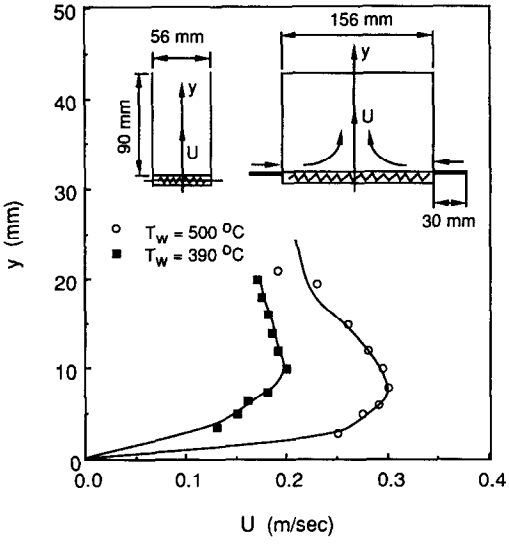

FIG. 4. Velocity profiles above the horizontal hot surface.

diameter), a high voltage (2–8 kV) was applied between a hypodermic needle and the hot plate to dislodge the suspended droplet from the capillary tip. This apparatus was adopted from the one developed in ref. [15]. For the droplet used in this experiment, the Weber number is between 1 and 10 which is much smaller than the threshold of $We = 30$ for sphericity. In the present study, the droplet generator was fixed at around 26 mm above the plate surface, resulting in a maximum impinging velocity of 0.4 m s^{-1} at room temperature. For a smaller droplet, the generating frequency is varied between 0.7 and 22 Hz so that the interval between two droplets is longer than the lifetime of the droplet on the hot surface.

Conventional photographic methods used for most previous experiments on free droplet motion and gasification may not be able to record the history of very small droplets in detail. For example, the residence time for a droplet of 0.1 mm impinging on a hot surface can be as short as 0.1 ms. In order to achieve this kind of resolution, a visual system was developed by using a video camera together with a strobe flash which would slow the time scale of a stable-repeatable process and then record the process on video tape for subsequent analysis. If the frequency of droplet generation and the frequency of the flash is perfectly synchronized, the droplet will appear stationary. If the frequency of the flash is slightly less than the droplet generation frequency, the droplet will appear to descend slowly. One can show that

$$U_i/U_d = f_i/f_d \quad (1)$$

where subscript i denotes the image as it appears on the video and f_i is the frequency of the droplet image appearing on the screen which is the difference between droplet generation frequency and strobe frequency. For example, at a droplet generation frequency of 20 s^{-1} and a strobe frequency of 19.9 s^{-1}, the period of the droplet image appearing on the screen can be as long as 60 s. Furthermore, using the advanced frame control of the video system where the visual images can be displayed frame by frame at 1/30 s interval, the actual time interval between two images can be as short as 0.03 ms. Detailed analysis shows that the accuracy of time scale transformation depends only on the accuracy of f_d which is $\pm 1\%$. The magnification of the video camera with various extension tubes and lenses is in the range of 33–205 and the accuracy of the magnification factor is $\pm 2\%$.

For larger droplets, the lifetime of droplets is of the order of seconds, thus measurement directly by the video system with a time resolution of 1/30 s is satisfactory.

Figures 5–8 are typical examples of using the above techniques to record the history of a heptane droplet impinging on a hot surface at different surface temperatures. Figure 9 shows the typical measurement of trajectories of impinging droplets. Good repeatability of the trajectories for different impinging droplets on the screen demonstrates the capability of the present experimental technique.

3. EXPERIMENTAL RESULTS

The evaporation modes of a liquid droplet impinging on a hot surface have been investigated and droplet lifetimes have been measured. Table 1 is a summary of the range of experimental data including the types of liquids, drop sizes and plate temperatures. All experiments were performed at atmospheric pressure in air. Most of the droplet sizes were between 0.07 and 0.4 mm with some data in water and hexadecane where drop sizes were as large as 1.8 mm.

3.1. *Effect of wall temperature*

Figures 10–13 show typical experimental results of the evaporation lifetime of hexadecane, heptane,

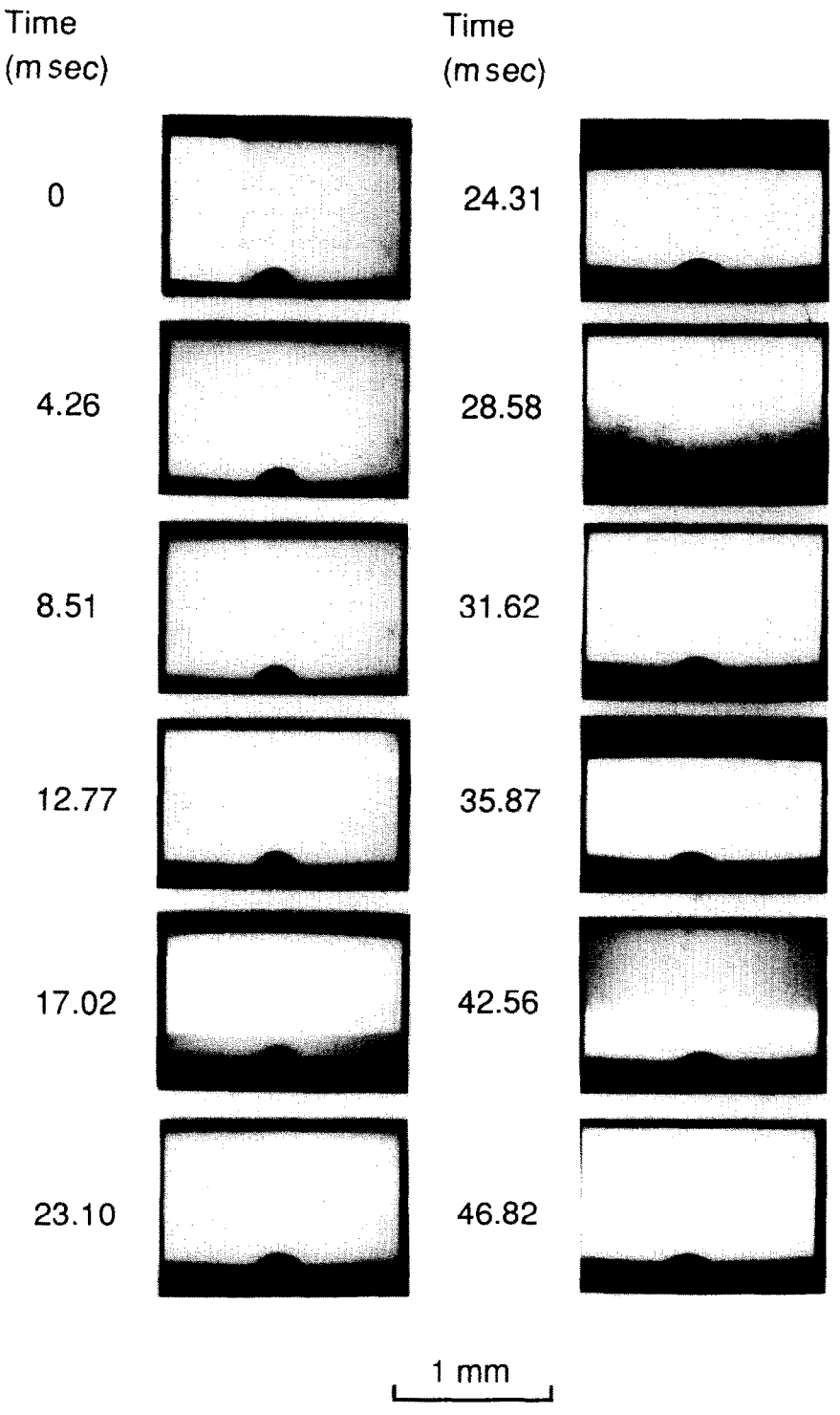

FIG. 5. Time history of a heptane droplet impinging on a hot surface at $T_w = 95°C$.

water droplets and diesel, respectively, as a function of wall temperature and drop sizes. Qualitatively the shapes of the curves are similar to that shown in Fig. 1.

For $T_w - T_b$ less than 20–30°C, droplets always adhere to the wall surface and attain a stable lens shape as shown in Fig. 5. Experimental measurement of fuel droplets shows that the configuration ratio of the height to the diameter of the 'drop lens' is close to a constant during most of the droplet lifetime except during the initial distortion period. An example of such a measurement for the case of hexadecane is shown in Fig. 14. Because the shape of the droplet resting on a surface depends on the equilibrium

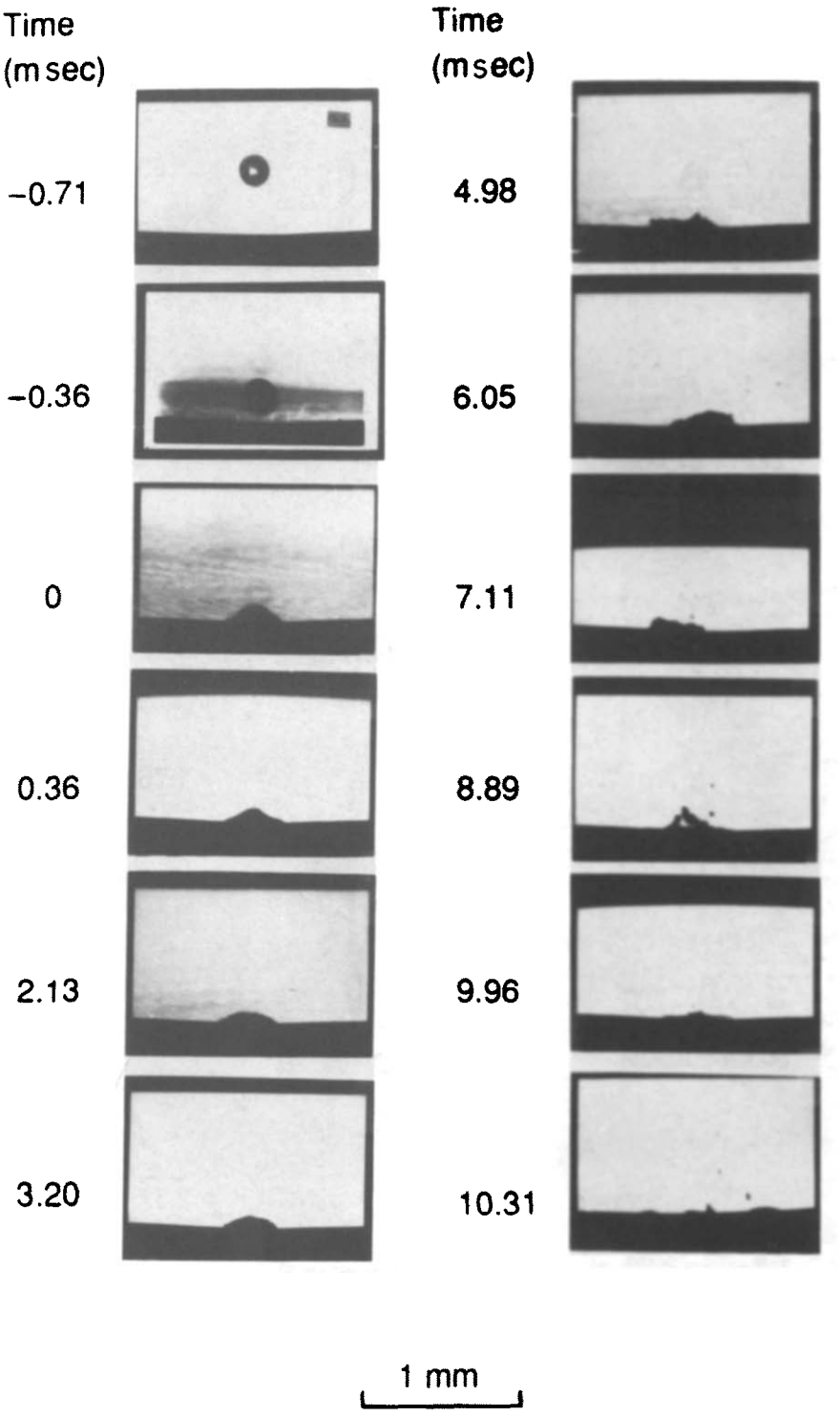

FIG. 6. Time history of a heptane droplet impinging on a hot surface at $T_w = 141°C$.

between gravity and the effects of its surface tension, Fig. 15 shows the correlation of $h/2a$ as a function of E_0 (Eotvos number) for selected hydrocarbon fuels. For the case of water, ref. [12] shows that for a larger droplet the wetted surface remains constant for most of the droplet lifetime. In this regime, heat conduction is the dominant mode of heat transfer. As a result, τ_e decreases rapidly with an increase in T_w. This is because both the temperature difference between the surface and the liquid and the wetted area of the droplet increase with T_w.

With increasing $\Delta T = T_w - T_b$, heat transfer intensifies notably due to liquid boiling. As T_w reaches a value of about 50–60°C above boiling which we

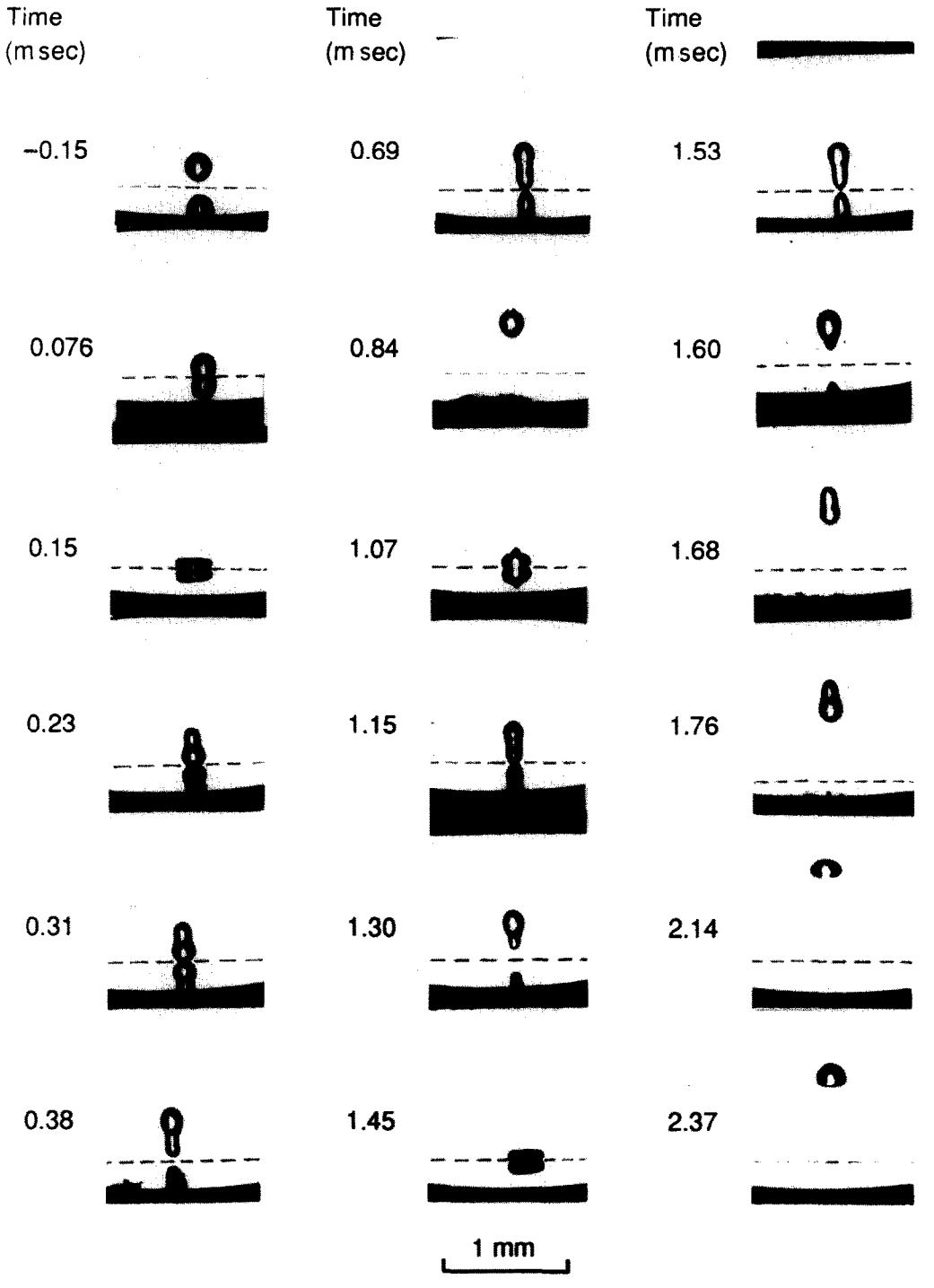

FIG. 7. Time history of a heptane droplet impinging on a hot surface at $T_w = 155°C$.

denote as $T_{w,c}$ rapid local boiling at the liquid–solid interface causes droplet distortion and ultimately disintegration, as shown in Fig. 6. The result of the disintegration of the droplet is almost instantaneous evaporation of all the liquid. Thus the evaporation lifetime τ_e approaches a minimum value which is of the order of several milliseconds depending on drop sizes and type of liquids. In this situation heat transfer rate reaches a maximum which can exceed the value of droplet burning in normal atmosphere. For example, the maximum evaporation rate, which can be estimated from D_0^2/τ_e is 4.4 $mm^2\ s^{-1}$ for a heptane droplet of 0.21 mm diameter and $T_{w,c}$ of 145°C, while the burning rate constant of a heptane droplet is only 1 $mm^2\ s^{-1}$. The values of $T_{w,c}$ of the present experiment as shown in Table 1 are generally about 10°C above the values shown in ref. [1].

For T_w exceeding $T_{w,c}$, τ_e increases drastically

Table 1. Summary of experimental data

Liquid	D_0 (mm)	T_w (°C)	Data size	T_b (°C)	$T_{w,c}$ (°C)	$T_{w,L}$ (°C)
Heptane	0.068–0.314	63–450	262	98	155	200–220
Octanol	0.142	148–550	72	195	258	295–315
Mesitylene	0.152	90–532	62	163	232	270–290
Hexadecane	0.094–1.40	166–570	335	287	335	390–430
Water	0.25–1.80	71–520	256	100	155	280–310
Diesel	0.191–0.422	200–605	230	—	356	430–440
Octanol (90%) Heptane (10%)	0.105–0.242	110–550	284	—	270	310–330

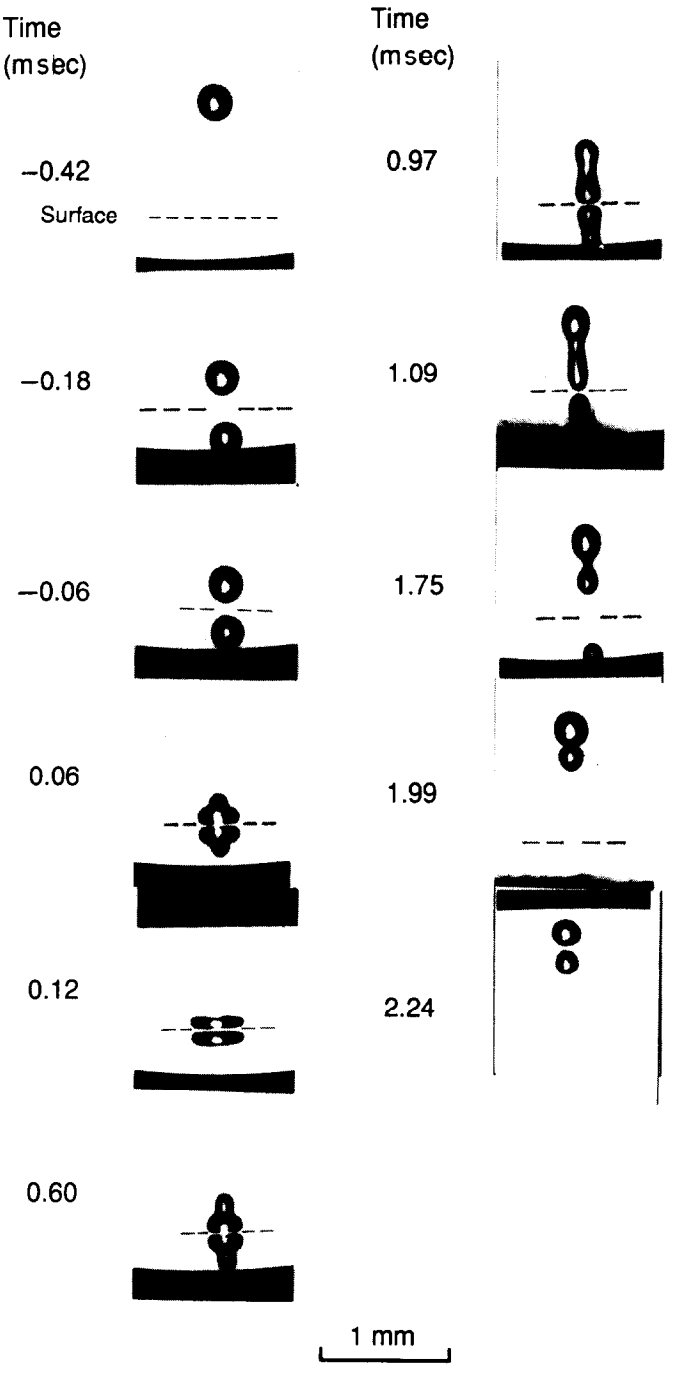

FIG. 8. Time history of a heptane droplet impinging on a hot surface at $T_w = 605°C$.

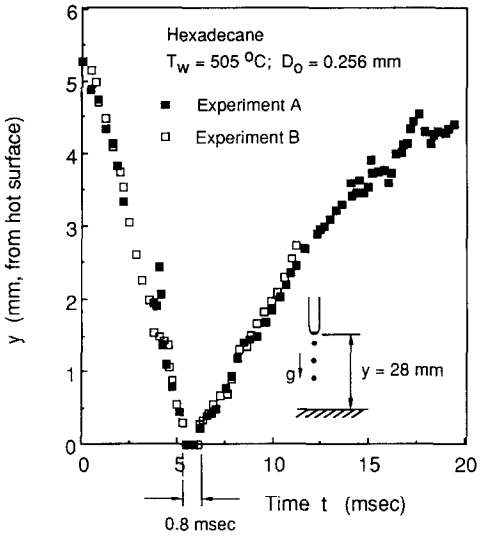

FIG. 9. Typical impinging droplet trajectory.

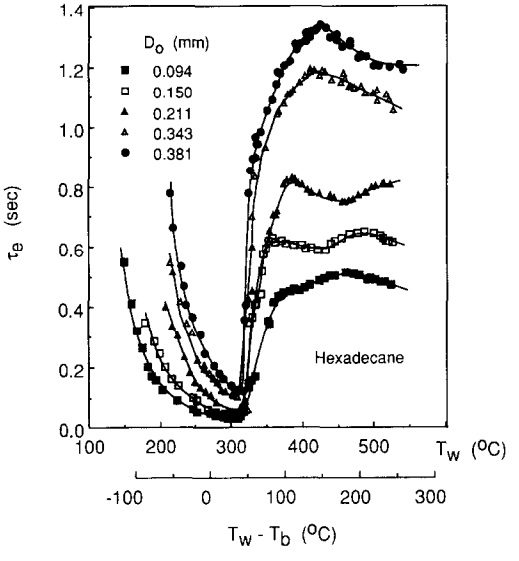

FIG. 10. Dependence of τ_e on D_0, T_w and $(T_w - T_b)$ for hexadecane droplets.

because the impinging droplet does not adhere to the surface but will start to bounce with increasing T_w. Observation shows that the larger droplets (diameter above 1 mm) barely bounce above the surface with a thin vapor film between the droplet and the surface. The dominant heat transfer mechanism is conduction. For a smaller droplet, however, diffusion–convection between the droplet and the environment plays a more important role because the droplet bounces many droplet diameters above the surface, as shown in Fig. 7. When $T_w - T_b$ approaches 100–120°C, τ_e attains a local maximum value in the transition mode for liquid fuels. For water, the local maximum τ_e corresponds to $T_w - T_b$ of approximately 180–210°C.

It has been found that for a larger droplet ($D_0 > 1$ mm) the Leidenfrost temperature $T_{w,L}$ is equal to 90–120°C above the boiling point of liquid fuels and 180–210°C above the boiling point for water. Thus the present data shows that the Leidenfrost temperature is mostly independent of drop sizes even for a mixture of fuels. The values of $T_{w,L}$ as shown in Table 1 for liquid fuels are generally 20°C higher than the values shown in ref. [1].

When $T_w > T_{w,L}$, the general trend for τ_e is to decrease as T_w increases for a larger droplet. This is because for a larger droplet, the droplet floats above the surface with a gap which is basically independent of T_w as long as $T_w > T_{w,L}$. Thus as T_w increases, both conduction and radiation heat transfer increase resulting in a decrease in τ_e.

For a smaller droplet which can bounce up and down many times and many diameters above the hot surface, the situation is complicated by the interactions of the droplet with the hot surface as well as the natural convection above the hot horizontal surface. As T_w increases, the induced air velocity above the hot surface increases which tends to keep the droplet away from the surface. Thus for a smaller droplet, τ_e tends to decrease only slowly or not at all with increasing T_w. In this situation, $T_{w,L}$ is not sharply defined. If the maximum induced air velocity reaches the terminal velocity of the falling droplet, the droplet may be stagnated much above the surface where the air temperature is quite low as shown in Fig. 3. As a result, the evaporation lifetime of the droplet may actually increase with T_w as shown in Figs. 10 and 11.

At very high T_w, mass efflux from evaporation is sufficient to prevent the droplet from physically touching the hot surface. This phenomenon is shown in the photographs of Fig. 8.

3.2. *Effect of liquid type*

To compare the lifetime of droplets of different liquids, Figs. 16 and 17 show typical data of τ_e vs $(T_w - T_b)$ of the same droplet size. The data show that $(T_{w,c} - T_b)$ and $(T_{w,L} - T_b)$ are about 55 and 110°C, respectively, for all fuels. Figure 16 shows that the maximum τ_e at $T_{w,L}$ is within 15% of each other for all fuels. This is because both the heat capacity and latent heat of vaporization are about the same for most hydrocarbon fuels. Since at $T_{w,L}$ evaporation time dominates the heating time, therefore τ_e remains the same for all fuels. On the other hand at $T_{w,c}$, heating time is more important because the droplet will disintegrate shortly after significant boiling occurs at the liquid–solid interface. Since heating time depends on both heat capacity and boiling temperature of the liquid, therefore fuels with the lowest boiling temperature would have the shortest τ_e as shown in Fig. 16 for heptane.

In the case of a mixture of heptane (10%)/octanol (90%), the data in Fig. 17 show that at $T_{w,L}$, τ_e of the mixture is slightly lower than both pure heptane and octanol, whereas at $T_{w,c}$, τ_e of the mixture is the same

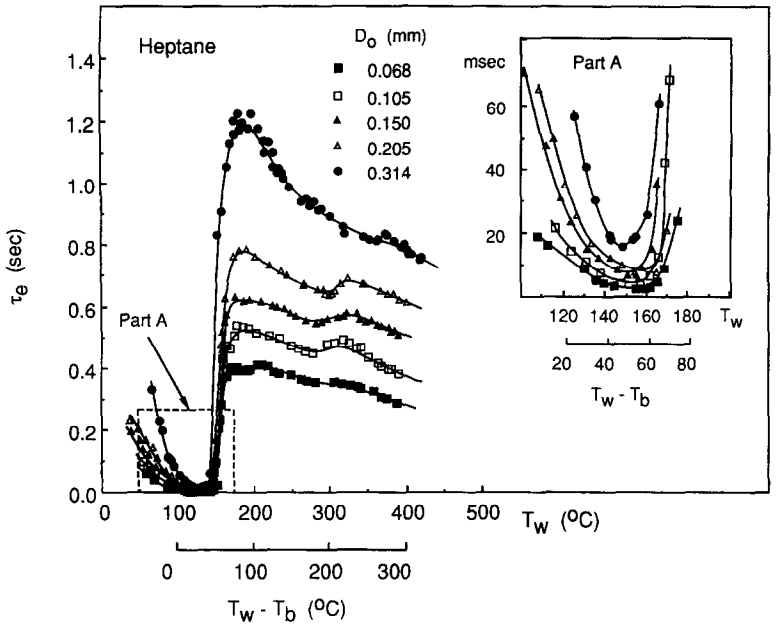

FIG. 11. Dependence of τ_e on D_0, T_w and $(T_w - T_b)$ for heptane droplets.

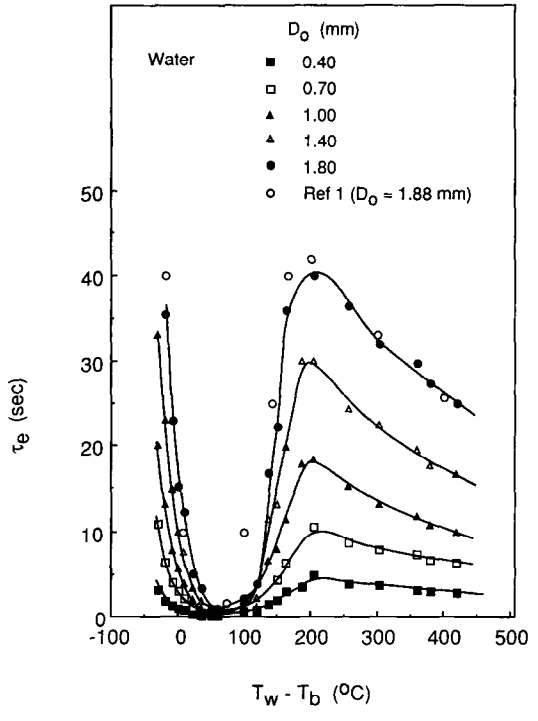

FIG. 12. Dependence of τ_e on D_0 and $(T_w - T_b)$ for water droplets.

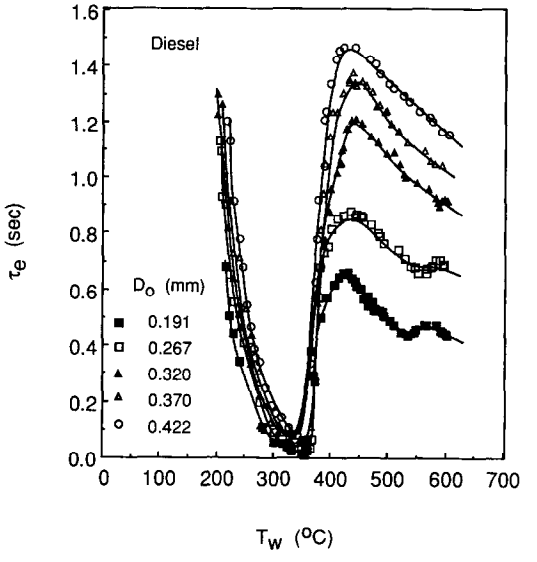

FIG. 13. Dependence of τ_e on D_0 and T_w for diesel fuel droplets.

as heptane. This is expected because the $T_{w,L}$ of the mixture is much higher than the $T_{w,L}$ of heptane and is quite close to the $T_{w,L}$ of octanol, thus the enhanced evaporation of heptane results in a lower τ_e. Similarly because $T_{w,c}$ of the mixture is much higher than the corresponding $T_{w,c}$ of heptane, rapid boiling of the heptane in the mixture would cause a rapid disintegration of the droplet.

Even for a blended fuel such as diesel fuel as shown in Fig. 13, the behavior of the τ_e vs T_w curves is very similar to the pure fuel. For example, the difference between $T_{w,L}$ and $T_{w,c}$ for diesel fuel is between 75 and 85°C which is well within the range of other pure hydrocarbon fuels.

Even though the τ_e vs $(T_w - T_b)$ curves are similar for hydrocarbon fuels, the curve of τ_e vs $(T_w - T_b)$ for water droplets is different. Figure 12 shows that for water droplets $T_w - T_b$ is around 180°C compared

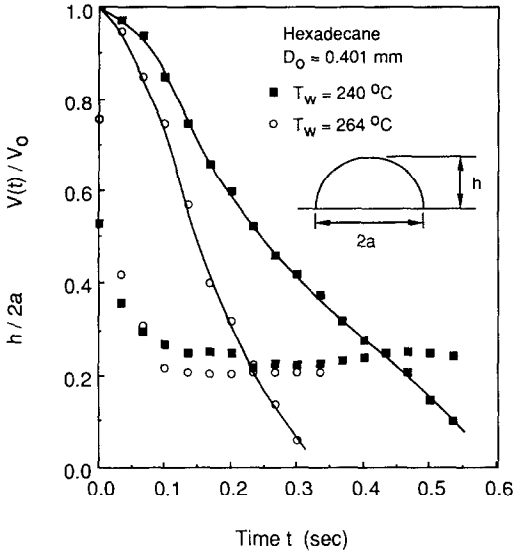

FIG. 14. Configuration ratio ($h/2a$) and volume variation ratio of droplets adhering to the hot surface.

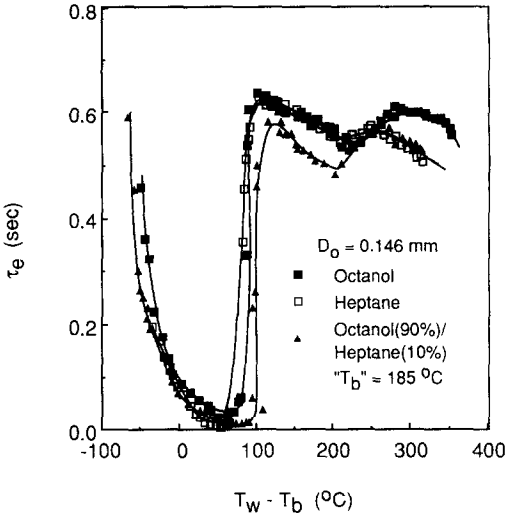

FIG. 17. Comparison of pure and mixed fuels of the same droplet size.

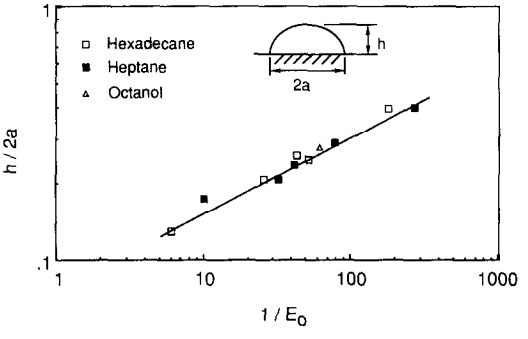

FIG. 15. Correlation of the configuration ratio ($h/2a$) as a function of Eotvos number $[g(\rho_l-\rho_g)D^{*2}/\sigma]$ where D^* is the equivalent diameter.

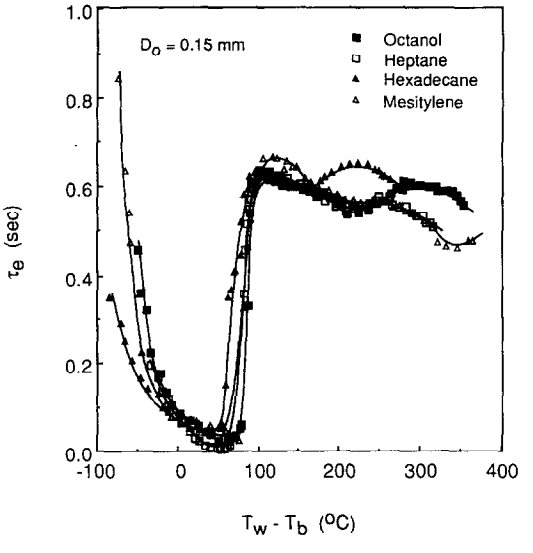

FIG. 16. Comparison of various fuels of the same droplet size.

with 120°C for hydrocarbon, and the transition from $T_{w,c}$ to $T_{w,L}$ for water droplets is much wider than that for hydrocarbon fuels. For the same drop size, the maximum τ_e for water is much larger than hydrocarbon fuels reflecting the larger value of the heat of vaporization of water.

3.3. *Effect of droplet size*

The previous data of droplet lifetime as a function of wall temperature can be replotted to show the effect of droplet sizes at a constant wall temperature. Typical plots for hexadecane, heptane and water are shown in Figs. 18–20, respectively. In a log–log plot of τ_e vs D_0, the slope of the curve represents the exponential factor n of D_0. Thus the data show that in all cases where the droplets adhere to the surface (film evaporation and nucleate boiling) or levitate close to the surface (larger droplet), the exponential factor n is between 1 and 2. For the smaller droplets in the transition and spheroidal evaporation modes, $n < 1$. The exact values of n depend on drop sizes, wall temperatures and the type of liquids.

It is well known from the D^2-law that for an isolated droplet evaporating in a quiescent atmosphere, τ_e is proportional to D_0^2. Thus the experimental data shows that the D^2-law is not valid for droplet–wall interaction.

In the case where the droplets either adhere to the surface or levitate close to the surface, heat transfer from the wall dominates. Thus, in a steady state, n should be close to 1. In a real situation, the unsteady effect may be important, radiative heat transfer and heat transfer from the cap to the droplet may be substantial, rendering n to be between 1 and 2.

A plausible reason why the smaller droplets in the transition and spheroidal modes have $n < 1$ is because

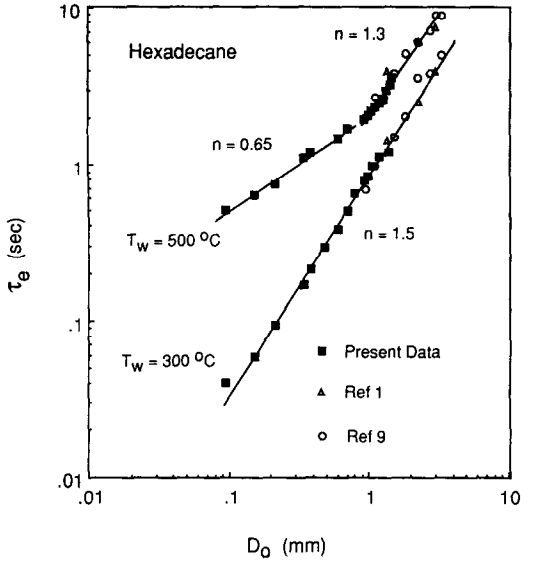

FIG. 18. Logarithmic plots of τ_e vs D_0 for hexadecane droplets.

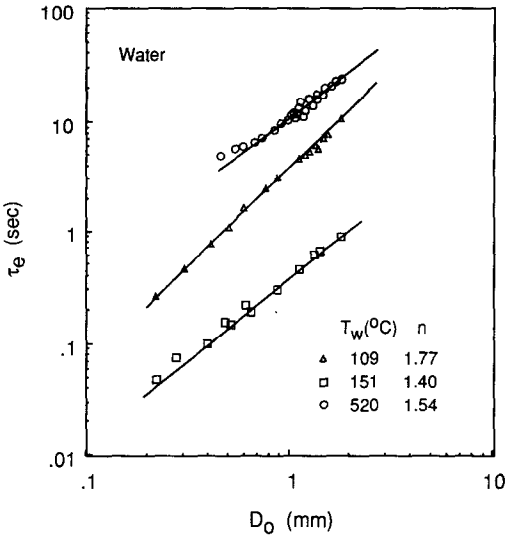

FIG. 20. Logarithmic plots of τ_e vs D_0 for water droplets.

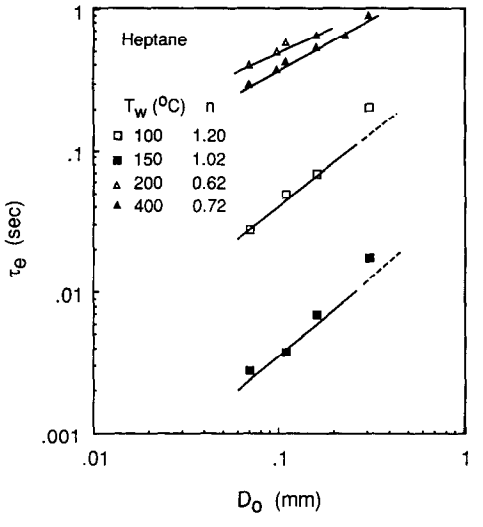

FIG. 19. Logarithmic plots of τ_e vs D_0 for heptane droplets.

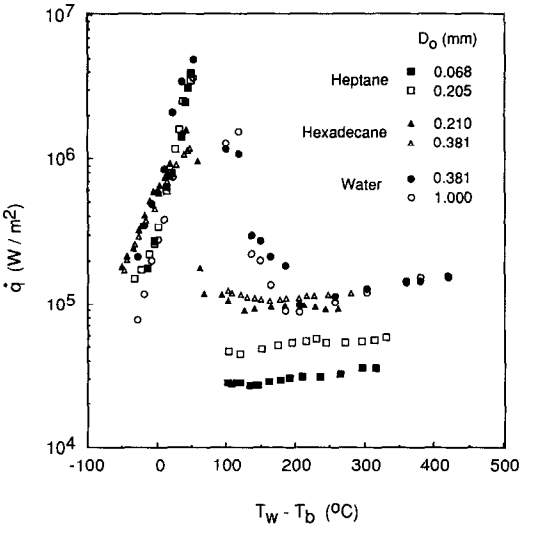

FIG. 21. Dependence of heat transfer rate $\dot{q}$ of heptane, hexadecane and water droplets on $(T_w - T_b)$.

there is a significant vertical temperature gradient near the wall surface. The smaller droplets which can bounce up to tens of diameters above the surface (function of diameters) experience a much cooler environment than those closer to the surface, thus it takes a relatively longer time to evaporate the smaller droplets. The net effect is the exponential factor $n < 1$.

Figure 18 shows a comparison of present data with that obtained by Tamura and Tanasawa [1] and Mizomoto *et al.* [9]. The results for larger droplets agree with each other.

3.4. *Heat transfer rate*

For the present problem, the average specific heat transfer rate $\dot{q}$, which is defined as the amount of heat transfer per unit cross-sectional area of the droplet per unit time, can be expressed as

$$\dot{q} = (2D_0\rho_1 H)/(3\tau_e) \quad (2)$$

where $H = L + C_p(T_d - T_\infty)$ is the effective heat of evaporation and the calculation of T_d is shown in the Appendix.

Figure 21 shows the dependence of $\dot{q}$ on wall temperature above boiling $(T_w - T_b)$ and initial drop size D_0 for heptane, hexadecane and water. As expected the data demonstrate that the maximum heat transfer rate $\dot{q}_{max}$, corresponding to the minimum lifetime of the droplet, appear at a wall temperature 50–60°C above the boiling point for all three types of liquids. Figure 21 also shows the $\dot{q}_{min}$ at Leidenfrost tem-

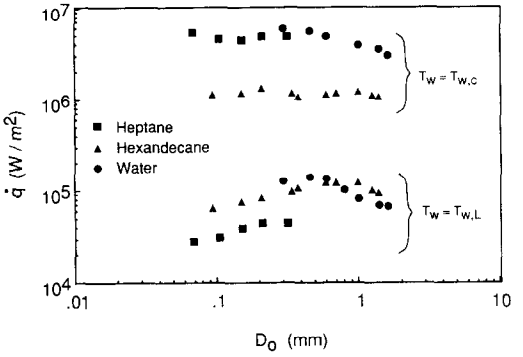

FIG. 22. Dependence of heat transfer rate $\dot{q}$ on droplet diameter D_0 at $T_{w,c}$ and $T_{w,L}$.

peratures which are roughly about 120°C above boiling for the fuels and 180°C above boiling for water.

To examine a little closer $\dot{q}_{max}$ at $T_{w,c}$ and $\dot{q}_{min}$ at $T_{w,L}$, we have plotted in Fig. 22 $\dot{q}$ as a function of D_0 at $T_{w,c}$ and $T_{w,L}$. The data show that $\dot{q}_{max}$ at $T_{w,c}$ for hexadecane is significantly lower than that for heptane and water. This is because basically $\dot{q}_{max}$ depends on the transient heating time of the droplet residing on the surface to be heated to the boiling temperature of the droplet. Since the boiling temperature of hexadecane is much higher than heptane and water, therefore $(\tau_c)_{min}$ is also higher resulting in lower $\dot{q}_{max}$. Figure 22 also shows that $\dot{q}_{max}$ is independent of D_0 for heptane and hexadecane which implies that n is equal to or close to 1. The water data shows a decreasing $\dot{q}_{max}$ with D_0 indicating that n is larger than one. At the Leidenfrost temperature $T_{w,L}$, for a larger droplet n is always larger than one, thus $\dot{q}$ decreases with increasing D_0. For smaller droplets where droplets can bounce ten or more diameters from the wall, n is smaller than one and thus $\dot{q}$ increases with increasing D_0. It appears that the maximum $\dot{q}$ occurs at about 0.5 mm diameter. At $T_{w,L}$ it appears that $\dot{q}$ for heptane is lower than that for hexadecane and water. A plausible explanation is that because $T_{w,L}$ of hexadecane which is about 400°C is much higher than that of heptane, which is at about 210°C, therefore radiation heat transfer renders $\dot{q}$ of hexadecane to be higher. In the case of water, because of the large heat of vaporization, the effect of vaporization is much less. Thus, for the same drop size, the water droplet will bounce with a much smaller amplitude thus experiencing a much higher temperature environment. As a result, $\dot{q}$ for water is higher that that for heptane at $T_{w,L}$.

4. CONCLUSION

The evaporation of a small liquid droplet impinging on a hot stainless steel plate has been investigated. The evaporation lifetime curves as a function of wall temperatures for several fuels, mixture of fuels and water have been obtained. Qualitatively the droplet lifetime curves as a function of wall temperature are similar for all liquids and all drop sizes. Quantitatively there are significant differences. The maximum heat transfer rate, which can significantly exceed the value of the burning droplet, occurs at 50–60°C above the boiling temperature for all pure liquids and Leidenfrost heat transfer rate, occurs at about 120°C for fuels and 180°C for water above boiling. Physically, beyond the maximum heat transfer point, larger droplets levitate above the surface whereas smaller droplets bounce up and down to many droplet diameters above the surface. Thus for the smallest droplets beyond the Leidenfrost temperature, τ_c actually increases with wall temperature which is in contrast to the larger droplets. The maximum heat transfer rate is independent of drop sizes for fuels and shows a slight decrease with increasing drop sizes in the case of water. At the Leidenfrost temperature, the data shows that the heat transfer rate is maximum at D_0 of approximately 0.5 mm.

REFERENCES

1. Z. Tamura and Y. Tanasawa, Evaporation and combustion of a drop contacting with a hot surface, Seventh Symp. (Int.) on Combustion, pp. 509–522 (1959).
2. C. S. Gottfried, C. J. Lee and K. J. Bell, The Leidenfrost phenomenon: film boiling of liquid droplets on a flat plate, *Int. J. Heat Mass Transfer* **9**, 1167–1187 (1966).
3. L. M. J. Wachters and N. A. J. Westerling, The heat transfer from a hot wall to impinging water drops in the spheroidal state, *Chem. Engng Sci.* **21**, 1047–1056 (1966).
4. R. W. Temple-Pediani, Fuel drop vaporization under pressure on a hot surface, *Proc Instn Mech. Engrs* **184**(38), 677–696 (1969).
5. G. S. Emmerson and C. W. Smoke, The effect of pressure on the Leidenfrost point of discrete drops of water and Freon on a brass surface, *Int. J. Heat Mass Transfer* **21**, 1081–1086 (1978).
6. S. Nishio and M. Hirata, Direct contact phenomenon between a liquid droplet and high temperature solid surface, PB-23, Sixth Int. Heat Transfer Conf., pp. 245–250 (1978).
7. M. Mizomoto, H. Hayano and S. Ikai, Evaporation and ignition of a fuel droplet on a hot surface (Part 1, Evaporation, Part 2, Ignition), *Bull. JSME* **21**, 1765–1779 (1978).
8. M. Mizomoto, H. Hayano and S. Ikai, Evaporation and ignition of a fuel droplet on a hot surface (Part 3, Effects of initial droplet diameter), *Bull. JSME* **22**, 1266–1273 (1979).
9. M. Mizomoto, H. Hayano and S. Ikai, Evaporation and ignition of a fuel droplet on a hot surface (Part 4, Model of evaporation and ignition), *Combust. Flame* **51**, 95 104 (1983).
10. K. Makino and I. Michiyoshi, The behavior of a water droplet on heated surfaces, *Int. J. Heat Mass Transfer* **27**, 781–794 (1984).
11. C. T. Avedisian and M. Fatehi, An experimental study of the Leidenfrost evaporation characteristics of emulsified liquid droplets, *Int. J. Heat Mass Transfer* **31**, 1587–1603 (1988).
12. M. di Marzo and D. D. Evans, Evaporation of a water droplet deposited on a hot high thermal conductivity surface, *ASME J. Heat Transfer* **111**, 210–212 (1989).
13. T. Y. Xiong, Dynamics and aerothermochemistry of interactive droplet vaporization and combustion, Ph.D. Thesis, Northwestern University (1986).

14. C. H. Wang, Combustion and micro-explosion of multi-component droplets, Ph.D. Thesis, Northwestern University (1983).
15. M. C. Yuen and L. W. Chen, On drag of evaporating liquid droplets, *Combust. Sci. Technol.* **14**, 147–154 (1976).
16. R. C. Reid, J. M. Prausnitz and T. K. Sherwood, *The Properties of Gas and Liquids*, 4th Edn. McGraw-Hill, New York (1987).

APPENDIX. CALCULATION OF DROPLET TEMPERATURE (T_d)

For quasi-steady spherical droplet evaporation in a quiescent atmosphere, the total mass flow rate can be shown to be

$$\dot{m} = \pi d_0 \rho_g \ln(1+B) \tag{A1}$$

where D_g is the binary diffusion coefficient, ρ the density and B the mass transfer number defined as

$$B = \frac{Y_d - Y_\infty}{1 - Y_d} \tag{A2}$$

where Y is the mass fraction.

For the present calculation, we shall assume that $\dot{m}$ can be calculated from the measured droplet lifetime τ_e by

$$\dot{m} = \rho_l \pi D_0^3 / 6\tau_e. \tag{A3}$$

Substituting equations (A2) and (A3) into equation (A1) and with $Y_\infty = 0$, one can then solve for the mass fraction of the vapor at the droplet surface in terms of τ_e and D_0. By assuming the mixtures of vapor and air as ideal gases, one can then solve for vapor pressure at the droplet surface as

$$p_{v,d} = (p_t Y_d)/(M_v)[Y_d/M_v + (1-Y_d)/M_a] \tag{A4}$$

where p_t is the total pressure and M the molecular weight. Finally, the droplet temperature is calculated from the Antonie equation

$$T_d = \frac{B_a}{A_a - \ln p_{v,d}} - C_a \tag{A5}$$

where A_a, B_a and C_a are Antonie coefficients as in ref. [16].

EVAPORATION D'UNE GOUTTELETTE DE LIQUIDE SUR UNE PLAQUE CHAUDE

Résumé—On étudie l'évaporation d'une gouttelette liquide frappant une plaque chaude en acier inoxydable. Les liquides sont l'eau, des combustibles hydrocarbures purs ou en mélange avec des tailles de goutte allant de 0,07 à 1,8 mm. Les températures de paroi varient de 63 à 605°C, couvrant le spectre complet des caractéristiques de transfert thermique entre l'évaporation en film (au dessous de la température d'ébullition) jusqu'à la vaporisation sphéroïdale (au dessus de la température Leidenfrost). Un système de visualisation stroboscopique-vidéo est utilisé pour enregistrer le mécanisme variable et pour mesurer la durée de vie de la goutte. Qualitativement, la courbe de durée de vie en fonction de la température de paroi est semblable pour tous les liquides et toutes les tailles de goutte. La densité de flux maximale se produit à 50–60° au dessus de la température d'ébullition pour tous les liquides purs et le point de Leidenfrost à environ 120°C pour les combustibles purs et 180° pour l'eau au dessus de la température d'ébullition. Le taux d'évaporation maximal peut excéder la vitesse de combustion des gouttelettes. Les visualisations montrent qu'au delà du point de transfert thermique maximal, les plus grosses gouttes se soulèvent au dessus de la surface tandis que les plus petites sautent et descendent de plusieurs diamètres. La densité de flux thermique maximale est indépendante des dimensions des gouttes pour tous les combustibles et elle décroît légèrement avec un accroissement de taille dans le cas de l'eau. A la température de Leidenfrost, les données montrent que la densité de flux thermique est maximale pour un diamètre de 0,5 mm environ.

VERDAMPFUNG EINES FLÜSSIGKEITSTRÖPFCHENS AUF EINER HEISSEN PLATTE

Zusammenfassung—Die Verdampfung eines kleinen Flüssigkeitströpfchens auf einer heißen Platte aus rostfreiem Stahl wird untersucht. Als Flüssigkeiten werden Wasser sowie verschiedene reine Kohlenwasserstoffe und Kohlenwasserstoffgemische verwendet. Die Tröpfchengröße liegt im Bereich von 0,07 bis 1,8 mm. Die Wandtemperaturen liegen im Bereich zwischen 63 bis 605°C und decken den gesamten Bereich der Wärmeübergangs-Mechanismen von der Filmverdunstung (unterhalb der Siedetemperatur) bis zur Verdampfung von Flüssigkeitskügelchen (oberhalb der Leidenfrost-Temperatur) ab. Ein Stroboskop/Video-System wird verwendet, um den zeitlich veränderlichen Prozeß aufzuzeichnen und um die Lebensdauer der Tröpfchen zu messen. Die Lebensdauerkurve der Tröpfchen in Abhängigkeit von der Wandtemperatur ist für alle Flüssigkeiten und für alle Tröpfchengrößen ähnlich. Der beste Wärmeübergang tritt bei allen reinen Flüssigkeiten 50–60°C oberhalb der Siedetemperatur auf, das Leidenfrost-Phänomen wird bei reinen, brennbaren Stoffen ungefähr 120°C und bei Wasser ungefähr 180°C oberhalb der Siedetemperatur beobachtet. Die maximale Verdampfungsrate kann die Verbrennungsrate von Kohlenwasserstofftröpfchen deutlich übersteigen. Visuelle Beobachtungen zeigen, daß oberhalb des Punktes für maximalen Wärmeübergang größere Tropfen auf der Oberfläche tanzen, während kleine Tröpfchen sich um bis zu mehrere Tröpfchen-Durchmesser über der Platte auf- und abbewegen. Das bedeutet, daß oberhalb der Leidenfrost-Temperatur die Lebensdauer kleinster Tröpfchen mit der Wandtemperatur zunimmt—im Gegensatz zu größeren Tropfen. Der maximale Wärmeübergang ist für alle brennbaren Stoffe von der Tropfengröße unabhängig und zeigt bei Wasser eine leichte Abnahme mit wachsender Tropfengröße. Bei der Leidenfrost-Temperatur zeigen die Meßwerte ein Maximum des Wärmeübergangs bei einem Tropfendurchmesser von ungefähr 0,5 mm.

ИСПАРЕНИЕ КАПЛИ ЖИДКОСТИ НА НАГРЕТОЙ ПЛАСТИНЕ

Аннотация—Исследуется испарение небольшой капли жидкости, ударяющейся о нагретую пластину из нержавеющей стали. В качестве жидкостей используются вода, различные чистые и смешанные углеводородные топлива с размером капли в диапазоне от 0,07 до 1,8 мм. Температуры стенки, изменяющиеся в пределах 63–605°С, охватывают весь спектр характеристик теплопереноса, от пленочного (ниже температуры кипения) до сфероидального испарения (выше точки Лейденфроста). Для регистрации нестационарного процесса и измерения времени жизни капли применяется стробоскопическая телевизионная визуализация. Кривая времени жизни капли как функция температуры стенки качественно аналогична для всех жидкостей и размеров капель. Максимальная скорость теплопереноса наблюдается при температурах, превышающих на 50–60°С точку кипения чистых жидкостей, а скорость теплопереноса, характерная для точки Лейденфроста, наблюдается при температурах, превышающих на 120°С точку кипения чистых топлив и на 180°С—точку кипения воды. Максимальная скорость испарения может значительно превышать скорость горения капель топлива. Визуальные наблюдения показывают, что за пределами точки максимального теплопереноса более крупные капли всплывают над поверхностью, в то время как мелкие подскакивают вверх на много диаметров над поверхностью и опускаются вниз. Таким образом, для капель минимальных размеров при температуре выше температуры Лейденфроста время жизни фактически возрастает с ростом температуры стенки, в случае же более крупных капель наблюдается обратная картина. Максимальная скорость теплопереноса для всех топлив не зависит от размеров капель и несколько снижается с увеличением их размеров в случае воды. Данные, полученные при температуре Лейдерфроста, показывают, что скорость теплопереноса достигает максимума при диаметре капли, равном, примерно, 0,5 мм.